JOURNAL OF SOLID STATE CHEMISTRY 20, 331–344 (1977)

The Microstructure of Slightly Substoichiometric NbO_2

J. R. GANNON AND R. J. D. TILLEY

School of Materials Science, University of Bradford, Bradford, West Yorkshire, BD7 1DP, England

Received August 31, 1976; in final form November 18, 1976

The microstructure of NbO_2 in samples of niobium oxides with bulk compositions lying between NbO and NbO_2 has been investigated by electron microscopy and X-ray diffraction. In oxygen-deficient samples NbO_2 possesses a complex microstructure which has been interpreted as being due to unmixing of two slightly substoichiometric forms of the oxide. One of these is of the rutile structure while the other was found to have a different symmetry characterized by the space group $P4_1$. The composition range of the NbO_2 phase was found to be at most from $NbO_{1.99}$ to $NbO_{2.034}$. No evidence was found to suggest that any nonstoichiometric variation in composition was accommodated by the presence of crystallographic shear planes.

Introduction

The salient features of the phases occurring in the niobium–oxygen system were reported by Brauer in 1941 (*1*). In the composition region between the oxides NbO and NbO_2 his original findings have remained largely unchanged by later studies (*2–4*) and materials with gross compositions lying between these oxides can be said to consist of biphasic mixtures of the dioxide and the monoxide if they are prepared at moderately high temperatures. The dioxide in particular was not reported to have any appreciable composition range, although one recent study states that the opposite is true (*5*).

This behavior is quite different from that of the closely related rutile structure oxides TiO_2 and VO_2. Earlier X-ray studies (*6*) indicated that well-defined homologous series of lower oxides Ti_nO_{2n-1} and V_nO_{2n-1} formed on reduction of the dioxide. Other studies suggested a broad homogeneity range for the MO_2 phase with a lower limit of about $MO_{1.90}$. However, recent investigations by electron microscopy (*7*) have revealed clearly that this composition variation near to MO_2 is due to poorly ordered or random arrays of crystallographic shear (*CS*) planes in the parent oxide which are not readily detected by X-ray diffraction until they order into the M_nO_{2n-1} series mentioned above.

Because of the close similarities between NbO_2 and these latter oxides, especially VO_2, and because of the fact that the higher niobium oxides related to Nb_2O_5 also contain *CS* planes it seemed profitable to study the microstructure of slightly reduced NbO_2 in biphasic mixtures of gross composition between the monoxide and the dioxide. Electron microscopy was used for this purpose, as *CS* planes are readily imaged by this technique and can be characterized even if present in only small numbers. In addition, the uncertainty about the stoichiometry range of NbO_2 merits clarification. This paper reports the results of the study which show that *CS* plane formation does not take place in NbO_2 and that the stoichiometry range of the dioxide is very small in samples quenched to room temperature.

Structure and Stoichiometry

In his original studies Brauer (*1*) did not determine the true unit cell of the dioxide

ISSN 0022-4596

TABLE I

POWDER X-RAY DATA FOR NbO_2[a]

Brauer (*1*)		Terao (*3*) $a_0 = 1.368_1$ nm $c_0 = 0.597_6$ nm		Magnéli (*8*) $a_0 = 1.371$ nm $c_0 = 0.5985$ nm		Marinder (*9*) $a_0 = 1.370$ nm $c_0 = 0.5987$ nm		This study,[b] $a_0 = 1.3699$ nm $c_0 = 0.5982$ nm		
d	*I*	*d*	*I*	*d*	*I*	*d*	*I*	*d*	*I*	*h k l*
		5.478	vw	5.495	vw	5.4976	vw	5.4781	vvw	1 0 1
								5.1008	vvw	1 1 1
		4.832	vvw							2 2 0
		4.283	vw	4.291	vw	4.2798	vw	4.2780	vvw	2 1 1
		3.628	w	3.631	w	3.6350	w	3.6367	vvw	3 0 1
3.484	vvw							3.4999	vw	3 1 1
3.408	vst	3.418	vst	3.425	st	3.4231	vst	3.4243	vst	4 0 0
3.353	vvw									4 1 0
3.213	vvw	3.206	w	3.211	w	3.2110	w	3.2098	vvw	3 2 1
		2.901	vvw	2.911	vw			2.9059	vvw	4 1 1
								2.8391	vw	3 3 1
2.588	vvw									5 2 0
2.544	vst	2.547	st	2.545	st	2.5456	vst	2.5435	vst	2 2 2
2.496	vvw	2.483	vw	2.494	w	2.4917	m	2.4927	vvw	5 0 1
2.420	st	2.419	m	2.425	m	2.4217	st	2.4222	mst	4 4 0
		2.338	vw	2.343	vw	2.3411	vvw			5 2 1
2.251	w	2.250	m	2.256	w	2.2546	st			4 0 2
								2.2214	vvw	4 1 2
								2.1806	vw	5 3 1
2.168	vvw	2.165	m	2.169	vw	2.1668	vw	2.1635	vw	6 2 0
		2.102	vvw			2.1079	vvw	2.1031	vvw	6 1 1
		2.012	vw	2.017	vvw					5 4 1
1.978	vvw	1.975	vw	1.977	vw	1.9754	m			1 0 3
1.939	vvw	1.926	vvw	1.935	vw	1.9338	w	1.9307	vvw	6 3 1
1.900	vw	1.897	vw	1.899	vw	1.8977	m	1.8938	vvw	2 1 3
1.864	vw	1.857	vw	1.864	vw	1.8610	m	1.8565	vvw	7 0 1
		1.825	vw	1.831	vw	1.8286	vw			3 0 3
1.798	vw	1.792	w	1.798	w	1.7958	m	1.7921	vw	7 2 1
				1.768	vw	1.7669	w			3 2 3
1.756	vst	1.753	st	1.756	st	1.7549	vst	1.7518	vst	6 2 2
1.735	vw									5 4 2
1.713	m	1.709	m	1.714	m[c]	1.7127	st	1.7101	mst	8 0 0
		1.685	vw							6 5 1
1.640	vw	1.632	vw			1.6350	m	1.6316	vvw	8 1 1
1.616	vw	1.612	vw			1.6136	m	1.6092	vu	5 0 3
1.572	vw	1.571	vw			1.5707	m			5 2 3
						1.5486	vvw			8 3 1
1.535	mw	1.529	m			1.5319	st	1.5267	mst	8 4 0
1.500	w	1.494	w			1.4967	st	1.4896	mw	0 0 4

[a] The indices are based on the cell dimensions of Marinder (*9*) using space group $P4_1$.
[b] Measured from an X-ray film of a sample of gross composition $NbO_{1.929}$.
[c] End of data quoted by Magnéli (*8*).

NbO_2 but he did point out that the structure was closely related to the rutile type. A decade later, Magnéli, Andersson, and Sundkvist (*8*) were able to index the X-ray powder photograph of NbO_2 in terms of a tetragonal unit cell which was reported to be a supercell of the rutile type, in accord with Brauer's results. The exact relationship between the NbO_2 structure and the rutile structure was clarified by Marinder (*9*) who determined the crystal structure of the niobium phase and showed that it contained pairs of niobium atoms united by niobium–niobium bonds. The arrangement of the metal atom pairs results in the larger cell observed in earlier studies. Despite this structure determination a comparison of published diffraction data of Brauer (*1*), Magnéli *et al.* (*8*), Marinder (*9*), and Terao (*3*) reveals inconsistencies, especially with respect to the existence of reflections which should be extinct according to the space group determined by Mariner (*9*) (see Table I).

At higher temperatures, above about 1080°K, the structure transforms to the normal rutile structure type (*10–13*). This structural change is also associated with changes in the electrical and magnetic properties (*14–19*) which has been interpreted as being due to disruption of the Nb–Nb pair bonds at high temperatures. Numerous related studies on ternary systems $M_xNb_{1-x}O_2$ have substantiated this conclusion. NbO_2 therefore shows quite close analogies with the related oxide VO_2.

The structure of NbO was derived by Brauer (*1*) and subsequently confirmed by a number of other studies including those by Andersson and Magnéli (*20*) and by Bowman *et al.* (*21*). The structure of NbO is unique among MO oxides in that the niobium atoms are coordinated to only four oxygen atoms in a square planar array. The structure is frequently described as being of the rocksalt type with one-quarter of both the anion and cation sites vacant although such a description is misleading as it implies that the NbO structure contains a high density of point defects.

The stoichiometry ranges of both NbO and NbO_2 have been reported to be very narrow. Brauer's results (*1*) indicate that they are virtually line phases and this has been borne out by later results (*2–4*). For example, the metal to oxygen stoichiometry range of NbO has recently been quoted as varying from $NbO_{0.98}$ to $NbO_{1.03}$ (*22*) at room temperature. Similarly the phase range of NbO_2 has been reported as having limits of $NbO_{1.9975}$ to $NbO_{2.0030}$ at 1373°K (*15*) and $NbO_{2.000}$ to $NbO_{2.2024}$ at 1573°K (*12*). Using solid-state galvanic cells, Alcock, Zador, and Steele (*23*) reported that the oxide NbO_2 was oxygen deficient, with a highest composition very close to NbO_2, but they do not quote definite limits. The only report to suggest that NbO_2 has a substantial composition range is that of Shin, Halpern, and Raccah (*5*) who propose composition limits of $NbO_{2.10}$–$NbO_{1.90}$ based upon thermogravimetric analysis, X-ray Laue photography, and electrical resistivity.

Experimental

Samples of niobium oxides with nominal compositions between NbO and $NbO_{2.1}$ were prepared by mixing together Nb and Nb_2O_5 powders of Specpure quality supplied by Johnson Matthey Ltd. The mixtures were compressed into pellets and the majority arc melted under an argon atmosphere. Some of the arc-melted samples were sealed in evacuated silica ampoules either alone or wrapped in molybdenum foil and annealed over a range of temperatures from 673°K upward for times of up to 13 weeks. The other samples were simply sealed into evacuated quartz tubes without being melted and heated at temperatures of up to 1373°K for times up to 7 weeks in duration. These preparations are detailed in Tables II and III.

Accurate compositions of each of the samples were obtained by controlled oxidation, at 873°K, on a Sartorius model 4102 microbalance. All the samples were X-rayed using a Guinier–Hägg focusing camera, with monochromatic Cu$K\alpha_1$ radiation, using KCl (a = 0.62923 nm) as an internal standard. The lattice parameters were refined using least-squares techniques (*24*). Electron microscope samples were prepared by crushing the pellets in an agate mortar and dispersing the fine fracture fragments in *n*-butanol. A drop of

TABLE II

SAMPLE PREPARATION AND X-RAY PHASE ANALYSIS

Composition	Preparation conditions[a]	Phases present
$NbO_{2.042}$	A	NbO, $NbO_2(P4_1)$, $Nb_{12}O_{29}$
$NbO_{2.025}$	A	NbO, $NbO_2(P4_1)$, $Nb_{12}O_{29}$
$NbO_{2.016}$	A	NbO, $NbO_2(P4_1)$, $Nb_{12}O_{29}$
$NbO_{1.929}$	A, M	NbO, $NbO_2(P4_1)$
$NbO_{1.915}$	S_2	NbO, $NbO_2(P4_1)$
$NbO_{1.846}$	A, S_6	NbO, $NbO_2(P4_1)$
$NbO_{1.826}$	P	NbO, $NbO_2(P4_1)$
$NbO_{1.816}$	S_2	NbO, $NbO_2(P4_1)$
$NbO_{1.813}$	S_3, S_4, S_5	NbO, $NbO_2(P4_1)$
$NbO_{1.740}$	S_2	NbO, $NbO_2(P4_1)$
$NbO_{1.707}$	A, M	NbO, $NbO_2(P4_1)$
$NbO_{1.591}$	A	NbO, $NbO_2(P4_1)$
$NbO_{1.588}$	S_2	NbO, $NbO_2(P4_1)$
$NbO_{1.516}$	S_2	NbO, $NbO_2(P4_1)$
$NbO_{1.506}$	A, M	NbO, $NbO_2(P4_1)$
$NbO_{1.497}$	A	NbO, $NbO_2(P4_1)$
$NbO_{1.340}$	A	NbO, $NbO_2(P4_1)$
$NbO_{1.170}$	A, M	NbO, $NbO_2(P4_1)$
$NbO_{1.109}$	A	NbO, NbO_2

[a] A = Arc melted only. M = Arc melted and annealed in molybdenum at 1073°K, 6 weeks. S_1 = Arc melted and annealed in silica at 1373°K, 1 week. S_2 = Arc melted and annealed in silica at 1273°K, 2 weeks. S_3 = Arc melted and annealed in silica at 1073°K, 6 weeks. S_4 = Arc melted and annealed in silica at 873°K, 6 weeks. S_5 = Arc melted and annealed in silica at 673°K, 6 weeks. S_6 = Arc melted and annealed in silica at 1373°K, 13 weeks. P = Sintered in silica at 1228°K, 7 weeks.

TABLE III

SAMPLE COMPOSITIONS AND X-RAY PHASE ANALYSIS FOR SOLID STATE PREPARATIONS IN THE RANGE $NbO_{1.92}$–$NbO_{2.08}$

Pellet composition		Phases present	
Nominal	Determined by oxidation	Pellet	Transported material
$NbO_{2.08}$	$NbO_{2.0347}$	$NbO_2(I4_1/a)$	$Nb_{12}O_{29}$
$NbO_{2.06}$	$NbO_{2.0340}$	$NbO_2(I4_1/a)$	$Nb_{12}O_{29}$
$NbO_{2.04}$	$NbO_{2.0352}$	$NbO_2(I4_1/a)$	$Nb_{12}O_{29}$
$NbO_{2.02}$	$NbO_{2.0348}$	$NbO_2(I4_1/a)$	$Nb_{12}O_{29}$
$NbO_{2.01}$	$NbO_{2.0329}$	$NbO_2(I4_1/a)$	$Nb_{12}O_{29}$ + $NbO_2(I4_1/a)$
$NbO_{2.00}$	$NbO_{2.0304}$	$NbO_2(I4_1/a)$	$Nb_{12}O_{29}$ + $NbO_2(I4_1/a)$
$NbO_{1.99}$	$NbO_{1.9965}$	$NbO_2(P4_1)$	None
$NbO_{1.98}$	$NbO_{1.9906}$	$NbO_2(P4_1)$ + NbO	None
$NbO_{1.96}$	$NbO_{1.9707}$	$NbO_2(P4_1)$ + NbO	None
$NbO_{1.94}$	$NbO_{1.9556}$	$NbO_2(P4_1)$ + NbO	None
$NbO_{1.92}$	$NbO_{1.9228}$	$NbO_2(P4_1)$ + NbO	None

this suspension was allowed to dry on a perforated carbon film. Examination was carried out using a JEM 100B electron microscope fitted with a goniometer stage and operated at 100 kV. Intensity measurements on both X-ray films and on electron micrographs were made using a Joyce Loebl double-beam recording microdensitometer.

Results

X-Ray Diffraction

A casual interpretation of the X-ray diffraction patterns of arc-melted material showed them to be in complete agreement with the literature, that is, samples with compositions below NbO_2 could be interpreted in terms of biphasic mixtures of NbO and NbO_2 while X-ray films from samples with compositions slightly above NbO_2 could be completely indexed in terms of $Nb_{12}O_{29}$ (*25*), NbO_2, and sometimes of NbO (see Table II). Not all the samples were homogeneous or at equilibrium, but the X-ray data taken as a whole indicate no appreciable stoichiometry range for either NbO_2 or NbO. Indeed, the lattice parameters of NbO_2, $a = 1.3699 \pm 2$ nm, $c = 0.5982 \pm 2$ nm, and of NbO, 0.4220 ± 2 nm did not change significantly in any of the X-ray films of samples from the whole composition range studied and are in good agreement with the literature values (*9*, *20*).

A closer examination of the X-ray films, however, particularly from samples with bulk compositions between NbO_2 and $NbO_{1.7}$ after subtraction of the lines attributed to NbO, showed weak extra lines which were not expected on the basis of the space group proposed for NbO_2 by Marinder (*9*), $I4_1/a$, No. 88. These weak lines were of variable intensity and sometimes only one or two were faintly visible. This was usually the case when the NbO_2 was present in nonequilibrium samples together with $Nb_{12}O_{29}$ and NbO. A more exhaustive examination of X-ray films ultimately showed that in annealed biphasic samples of NbO_2 and $Nb_{12}O_{29}$ the NbO_2 gave powder patterns identical to that reported by Marinder (*9*) but as the overall composition of the samples fell, the weak lines became readily visible.

In order to check whether these faint lines were due to a previously unreported niobium oxide an extensive series of preparations were made and annealed at temperatures down to 673°K for as long as 13 weeks. In none of these could the weak lines be intensified at the expense of the NbO_2 or NbO lines present.

In addition to this failure to produce substantial quantities of a phase which gave rise to these weak reflections alone, it was also found impossible to index them satisfactorily on a new unit cell. However, every one of these lines could be assigned indices in terms of a unit cell of the same dimensions as that proposed by Marinder (*9*), provided that the space group restrictions were lifted. Table I records all such indexed lines present on an X-ray film of a sample of gross composition $NbO_{1.929}$ annealed for 6 weeks at 1073°K. all other lines on the film were attributable to NbO. A comparison with the literature data presented in Table I shows that some of these weak lines have, in fact, been reported in the past as being NbO_2 reflections.

The modified space group was derived from a consideration of the indices of observed lines on X-ray films from samples with overall compositions slightly below NbO_2. Referring to Table I one can note that the presence of (111) and (311) reflections rule out a body- or face-centered lattice and indicate a primitive tetragonal lattice. The presence of the (004) reflection leads to the conclusion that the most likely space group is $P4_1$, No. 76. Such a space group is in accord with the reflections observed in the electron diffraction patterns as well as the X-ray films. Using the above information it was now found to be possible to completely index the X-ray powder data for NbO_2 quoted in all previous studies, and these are shown in Table I.

An examination of the X-ray patterns of those samples prepared by solid-state reaction with nominal compositions close to NbO_2 confirmed that the stoichiometry range of this phase is rather limited. A consideration of the X-ray phase analysis of these samples, presented in Table III, shows that the lower limit of the stoichiometry range, characterized by the appearance of reflections from NbO on the X-ray film, lies somewhere between the com-

positions $NbO_{1.997}$ and $NbO_{1.990}$. For samples more oxygen rich than NbO_2, disproportionation via vapor transport occurred. The compositions of the residual pellets were quite close to one another, with a mean value of $NbO_{2.0336}$ and a standard deviation of 0.0017. The transported material was, in each case, $Nb_{12}O_{29}$. This indicates that the upper composition limit of NbO_2 must be close to $NbO_{2.034}$.

No significant change in the lattice parameter of NbO_2 was detected as this composition range was spanned and every X-ray reflection could be indexed in terms of the phases detailed in Table III.

Electron Microscopy

Although all the samples listed in Tables II and III were carefully examined by electron microscopy, no evidence was found to suggest that either ordered or disordered *CS* planes were present, and diffraction patterns never showed large unit cells that could have derived from ordered arrays of *CS* planes. No differences were found between melted and nonmelted samples from this point of view and it was concluded that *CS* planes do not form in the NbO_2 structure under the conditions employed in these experiments.

The crystal fragments examined could initially be divided into two types, NbO and NbO_2. The reciprocal lattices of these two phases differ sufficiently for them to be distinguished although care must be taken not to confuse the *hk*0 section of NbO_2 with the *hk*0 section of NbO. These are compared in Fig. 1. The fragments identified as NbO always displayed electron diffraction contrast associated with unfaulted ("perfect") crystals. They were found in all samples up to and including those with a bulk composition of $NbO_{1.929}$. No apparent difference existed between NbO from samples at either end of the composition range.

The NbO_2 flakes were more complex in appearance. At the oxygen-rich end of the composition range studied they were unfaulted ("perfect") crystals from the point of view of electron diffraction contrast. However, reduced samples usually contained NbO_2 with a faulted structure which is more fully described below. This faulted structure existed in samples with bulk compositions as low as $NbO_{1.35}$, and was also found in the samples which were prepared by solid-state reaction of Nb_2O_5 and Nb, as well as those which were melted.

Fragments from samples in the middle and lower parts of the composition range frequently, but not always, contained precipitates in a host matrix of NbO_2. Sometimes these precipitates were large and exhibited complex

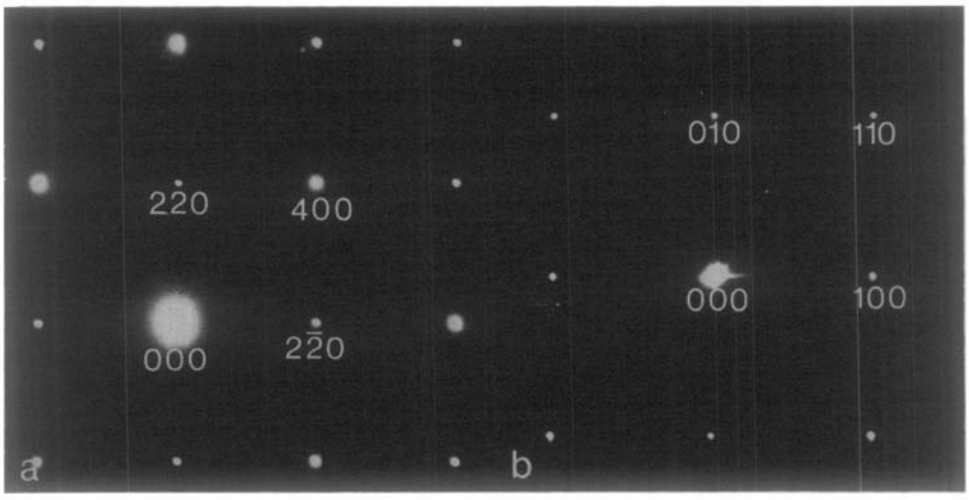

FIG. 1. (a) Diffraction pattern of the *hk*0 reciprocal lattice section of NbO_2. (b) Diffraction pattern of the *hk*0 reciprocal lattice section of NbO.

interfacial contrast while in other flakes they were small. The large precipitates were identified as NbO and the small ones are presumed to be the same. The electron diffraction contrast from these materials was typical of that from two-phase materials (*26*) and was not analyzed in depth. It was noted, however, that if a crystal fragment of NbO_2 contained precipitates of NbO it was always unfaulted and identical to those found in the samples at the oxygen-rich end of the composition range studied.

Crystal fragments from samples with bulk compositions lying between $NbO_{1.929}$ and $NbO_{1.707}$ were most often found to be of the faulted NbO_2 type not containing precipitates. The diffraction patterns associated with this faulted material were similar to those from NbO_2 fragments and, in particular, the $hk0$ sections were identical and of the sort shown in Fig. 1a. However, spots with $l \neq 0$ usually exhibited streaking either parallel to a^* or b^* as shown in Fig. 2. In addition, more spots were present on these upper reciprocal lattice layers than the space group of NbO_2 proposed by Marinder, $I4_1/a$, allowed, Moreover, a careful examination of the sequence of streaks on the upper layers of the reciprocal lattice revealed that not every spot was streaked, and that of the streaked spots, not every one was streaked in the same direction. A diagrammatic representation of the streaking pattern, built up from a number of diffraction patterns obtained by tilting the crystal fragments about the a^* axis, is shown in Fig. 3. As the a^* and b^* axes cannot be distinguished on the electron diffraction patterns it is concluded that a similar set of streaks (but with the directions parallel to and normal to a^* shown in Fig. 3 reversed) would be excited on tilting about b^*.

The faults themselves were difficult to image using electron diffraction contrast and it was found that annealed samples gave rather better contrast than the as-arc melted samples. This appears to be because the boundaries to the faults are sharper and more well defined in the annealed materials. As annealing progressed the faults became more clearly delineated until the contrast was that typical of thin lamellae of a twin or of a second phase with well-defined planar boundaries. Both of these extremes are shown in Fig. 4. In practice it was found that the faults were only visible

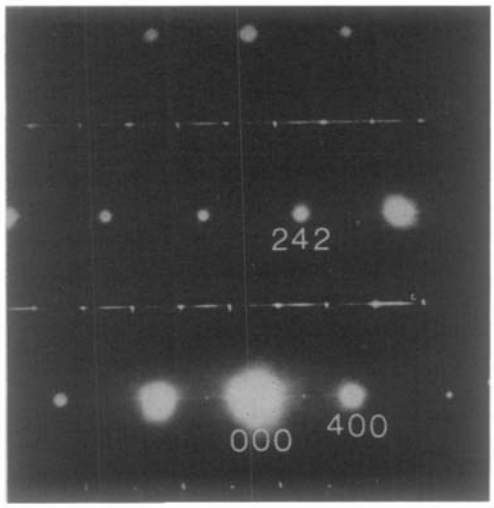

FIG. 2. Diffraction pattern taken from a faulted fragment showing the complex pattern of streaking parallel to a^*.

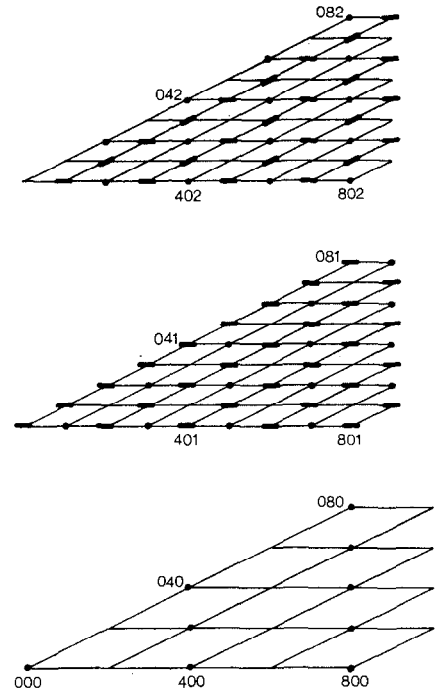

FIG. 3. Diagrammatic representation of the streaking pattern on the $hk0$, $hk1$ and $hk2$ reciprocal lattice layers of slightly substoichiometric NbO_2.

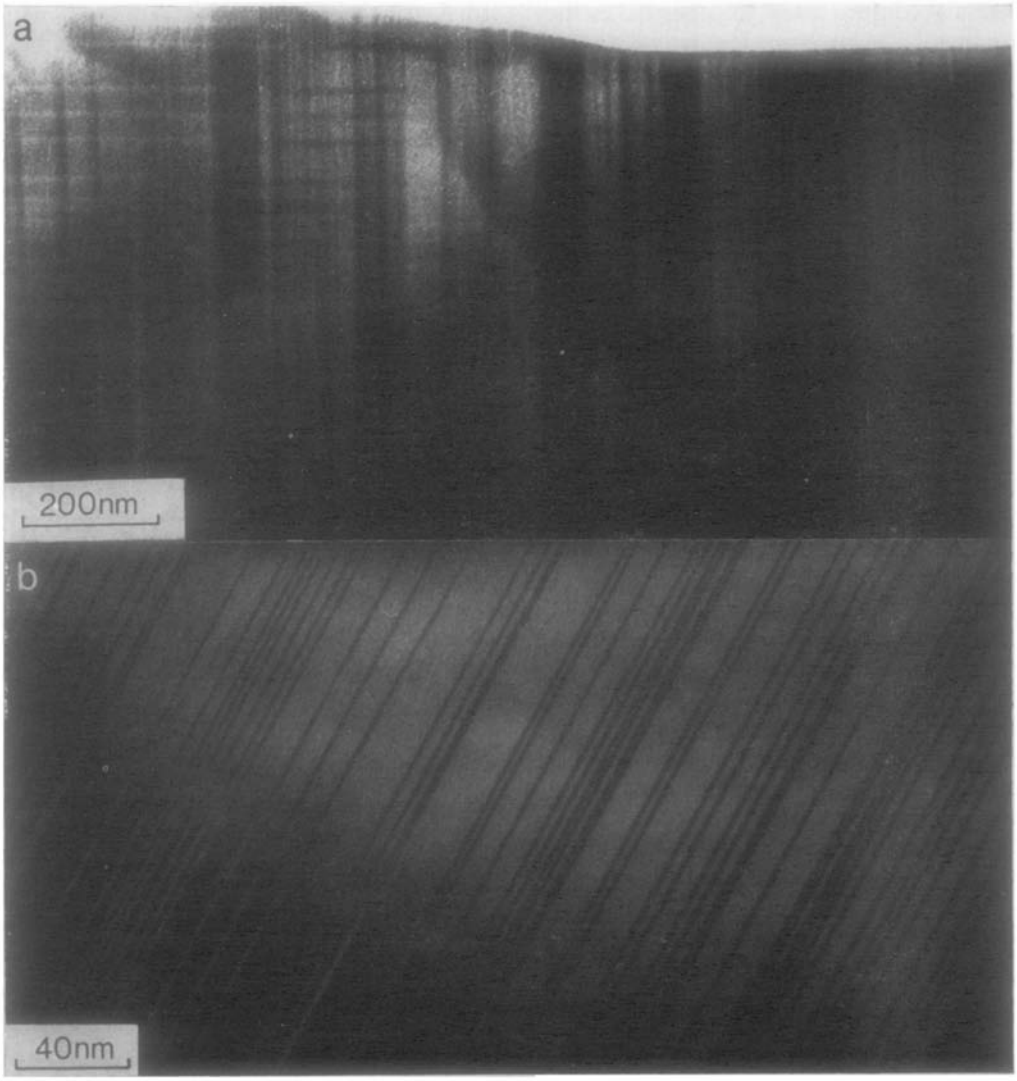

FIG. 4. (a) Micrograph taken from an arc-melted sample showing faults exhibiting poor interfacial contrast. (b) Micrograph taken from an annealed sample. The faults are sharper and more clearly delineated.

by diffraction contrast when streaked reflections with $l \neq 0$ were present on the diffraction pattern. A comparison of the streaking on the diffraction pattern with the fault directions on the micrographs, taking into account the relative rotation of diffraction patterns and micrographs, indicated that the fault planes were upon $\{h00\}$ or $\{0k0\}$ planes. As the $hk0$ reciprocal lattice section was unstreaked and the faults were invisible when crystal fragments were oriented with their c axes parallel to the electron beam, there was, however, the possibility of small angular errors in this assignment.

The faults were found to be quite stable in the electron beam but intense irradiation caused them to disappear rapidly. When this happened the material took on the appearance of unfaulted NbO_2. The reciprocal lattice became unstreaked and the only spots present were those which accorded with Marinder's space group $I4_1/a$. Sometimes the disap-

pearance of the faults was accompanied by the formation of small precipitates, as shown in Fig. 5, and sometimes not. The nature of the precipitates has not been studied in detail, but thermodynamic considerations would suggest that oxidation is a more likely process than reduction and they are assumed to be higher oxides. A more thorough study of this reaction would be of interest.

In order to clarify the nature of the faults in the slightly reduced samples of NbO_2, high-resolution electron micrographs were taken.

Tilting the crystal flakes about a^* sometimes caused the forbidden {200} spots to appear alone and at other times the {100}, {200}, and {300} spots were excited. The former type of diffraction pattern was more frequently observed in samples which were close in composition to NbO_2 and images formed using the {200} and {400} reflections revealed a set of continuous 0.34-nm fringes as shown in Fig. 6 where a modulation due to the superimposed 0.68-nm {200} fringes can be seen.

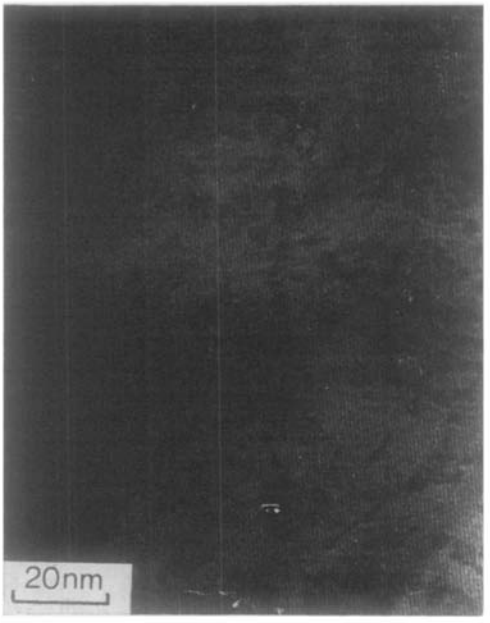

FIG. 5. Micrograph showing precipitates and continuous (110) fringes in NbO_2. The precipitates were induced by beam heating a faulted fragment of the type shown in Fig. 4a.

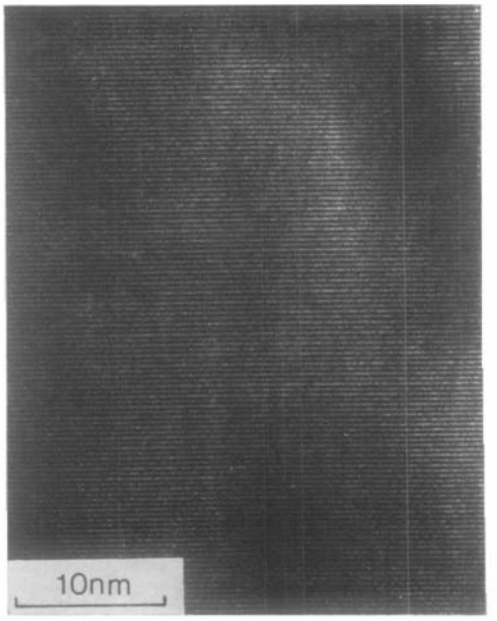

FIG. 6. Micrograph taken from a faulted fragment showing continuous 0.34-nm fringes with a modulation imposed by 0.68-nm fringes.

Images formed using the {100}, {200}, {300}, and {400} reflections, which were more often seen in samples with compositions around $NbO_{1.8}$, showed regions where 1.37-nm and 0.34-nm fringes were intergrown as shown in Fig. 7. A microdensitometer trace taken across the area shown in Fig. 7b reveals three fringe profile types which can be attributed to 0.34-nm fringes alone, 0.34- and 0.68-nm fringe intergrowths, and 0.34- and 1.37-nm fringe intergrowths. It appeared that samples which were more oxygen deficient contained a greater percentage of intergrowths between 1.37- and 0.34-nm fringes, these intergrowths being separated by areas containing 0.34-nm fringes only, or an intergrowth between 0.68 and 0.34-nm fringes. These micrographs also revealed that the center line of the faults was not exactly parallel to the (h00) fringes but were at a slight angle to them. This effect is shown in Fig. 8.

Crystal fragments were also tilted about the [110] direction to obtain further information. This tilting caused the {110} spots to intensity and produced 0.9-nm fringes in some areas of the crystal. Fig. 9a shows this effect and indi-

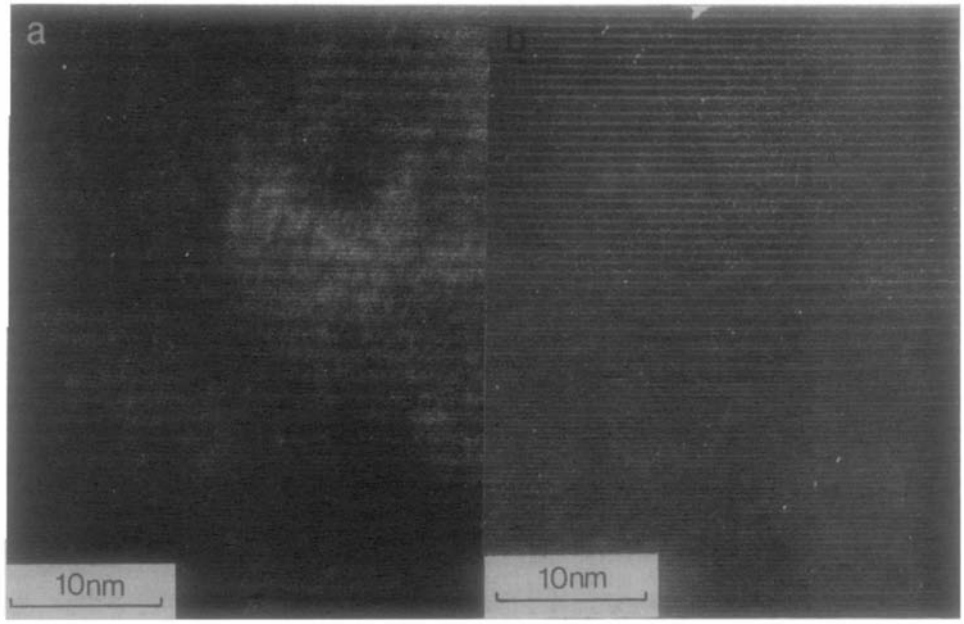

FIG. 7. (a) Micrograph showing 0.34-nm fringes with a modulation imposed by the 1.37-nm fringes in a faulted fragment. (b) Micrograph taken from a different region of the same fragment as (a). Here there is a band of 1.37-nm fringes bounded by regions of 0.68- and 0.34-nm fringe intergrowths. (c) Microdensitometer trace taken across the area shown in Fig. 8b showing three fringe profile types.

cates that the faulted regions are free of these fringes. If images are obtained using the {220} reflections when the {110} reflections are not strongly exited, no such difference is found, and the 0.45-nm {220} fringes are uninterrupted, although faults could be seen to exist in the crystal flake using diffraction contrast techniques. Such a micrograph is shown in Fig. 9b.

Interpretation

The faults observed in NbO_2 in contact with NbO cannot be interpreted as due to regions or lamellae of new oxide phases, such as a hypothetical Nb_2O_3. The reasons for this are that the extra reflections corresponding to such a new phase were never found in electron diffraction patterns and the material could not be prepared pure or even in such quantities as to give a unique X-ray diffraction pattern. Similarly, the faulted areas cannot be regions containing NbO in the form of lathe-like precipitates or intergrowths as it is impossible to fit the NbO_2 and NbO reciprocal lattices together so that all NbO spots are masked by NbO_2 reflections, and careful examination of the diffraction patterns of faulted materials never revealed any reflections other than those fitting the NbO_2 cell.

The X-ray analysis suggests that NbO_2 in contact with NbO contains variable amounts of a modification with a space group different from that proposed by Marinder (*9*), although with the same size of unit cell. An interpretation of the faulting in NbO_2 in contact with NbO that is in accord with this is to assume that the faults are lamellae of NbO_2 with different symmetries, completely intergrown with one another. The ultimate change would appear to be from NbO_2 ($I4_1/a$), described by Marinder (*9*), to NbO_2 ($P4_2/mnm$) with the rutile structure by way of an intermediate form of somewhat lower symmetry ($P4_1$). Such a change is physically reasonable. The $I4_1/a \rightarrow P4_2/mnm$ change is well documented (*10–13*) and only very small atomic shifts are needed to transform Marinder's $I4_1/a$ space group to $P4_1$.

The diffraction patterns from faulted flakes

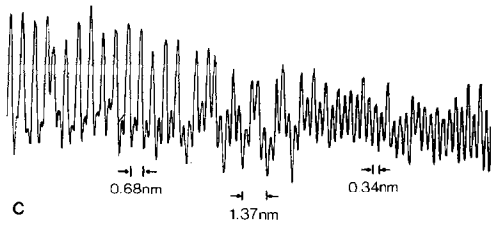

FIG. 7—*Continued*

are always of the low-symmetry $P4_1$ type and the results here suggest that this material is present in fair amounts when the faults are present. However, it is difficult to interpret the electron-diffraction patterns unequivocally in this respect, as double diffraction can easily lead to the presence of space group forbidden reflections, and dynamical effects add further to the difficulty of assessing the true (kinematical) intensity of a reflection. However, one can note that on tilting about a^* sometimes only the {200} spot appears while at other times the {200} spot is accompanied by the {100} and {300} reflections. If the material giving rise to just the {200} reflection is taken as being the $I4_1/a$ phase while the material giving rise to the {100} and {300} reflections is taken as the $P4_1$ phase, then the interpretation can be taken further. In this case, 0.68-nm fringes can be equated to the $I4_1/a$ structure, 1.37 nm to the $P4_1$ structure, and 0.34-nm fringes to the $P4_1/mnm$ (rutile) structure. Thus one can see that the $I4_1/a$ structure intergrows with both the rutile phase and with the lower-symmetry $P4_1$ phase, and this latter phase can also coexist with the rutile phase. Neither the $P4_1$ phase nor the rutile phase were found alone in fragments to any great extent. These suggestions are in agreement with the X-ray powder data, as the rather variable relative intensities of the lines would reflect the variable proportions of these phases in the samples examined. The intergrowths, taking the form of thin lamellae, would cause some lines to be broadened relative to others (*27*), resulting in the apparently slightly variable positions of these lines compared to the rutile lines.

The complex pattern of streaking shown in Fig. 3 arises from the intergrowth of these three structures. The rutile-type reflections are never streaked, since these exist for all three modifications, and, as is clear from the point of view of the atom planes giving rise to these reflections, the structure is unfaulted. Not all the remaining spots are streaked, and the

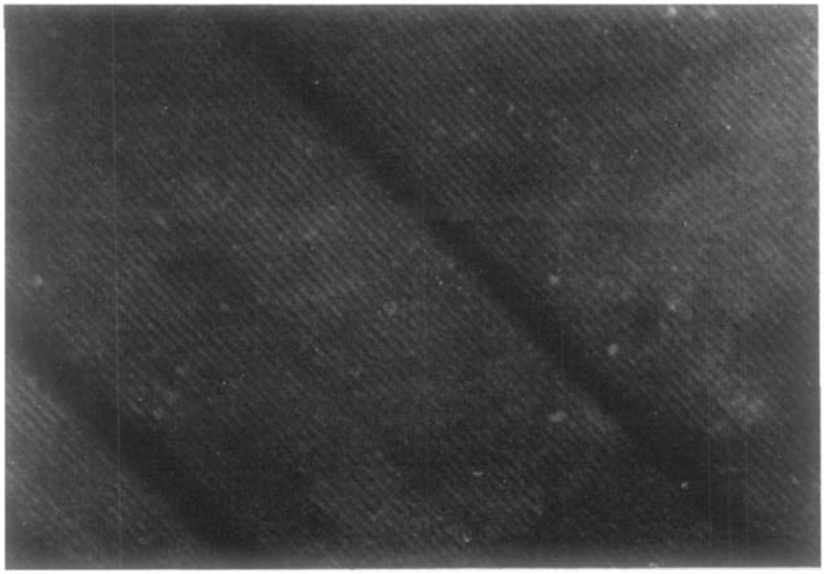

FIG. 8. Micrograph showing 1.37-nm fringes in some regions of a faulted fragment. The fringes can be seen to make a very small angle with the fault interfaces.

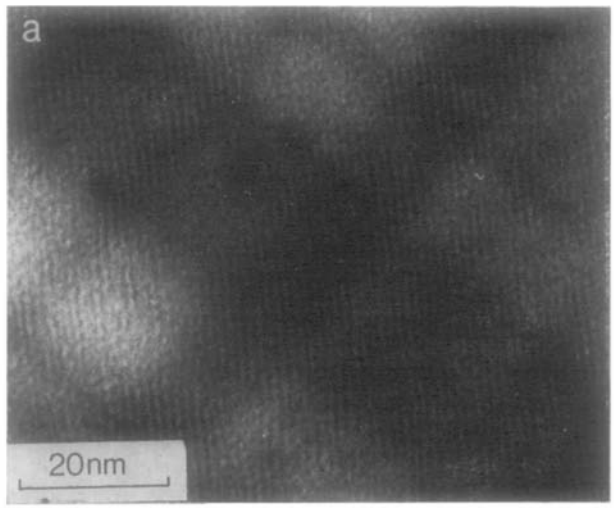

FIG. 9. (a) Micrograph showing discontinuous (110) fringes which are resolved at the intersections of perpendicular faults. (b) Micrographs showing continuous (220) fringes in a faulted fragment.

direction of streaking also depends upon the indices of the reflection.

The streaking may be treated from two points of view. Wilson (*27*) has discussed the formation of streaks on X-ray photographs due to materials with stacking mistakes and other faults. From his treatment it is clear that the present pattern cannot be simulated if the streaking is assumed to be caused by either a sinusoidal variation of structure factor in a direction perpendicular to the faults or by a sinusoidal variation in the lattice parameter, for, in both cases, all reflections should be affected. Similarly, the effect is not due to the "thin crystal" nature of the lamellae of the various structures making up each flake, as again, each spot should be affected equally. It would seem likely that a simultaneous variation in lattice parameter and structure factor, as would be expected, could explain the pattern. However, a fuller interpretation is not possible at present because the actual amplitudes of scattered electron waves are considerably different from the amplitudes predicted by kinematical theory, and because the exact atom positions in the phase of space group $P4_1$ are unknown. The second approach which may throw light on the problem of the streaking pattern is that of considering the symmetry constraints present in the crystal during transformation. This has been used by McConnell (*28*) to clarify phase separation in a number of minerals, and deals with the effect of distortion waves upon the diffracted intensities. As in the approach described above, a simple analysis does not explain the observed intensity distribution. It seems likely, therefore, that a complete explanation of the diffraction patterns will require a more extended series of observations, perhaps using X-ray diffraction in order to gain useful intensity data and treated by the general methods set out by Cowley (*29*).

Discussion

Taking the X-ray results alone, it is clear that neither NbO_2 nor NbO have appreciable stoichiometry ranges at room temperature, using both lattice parameter measurements and the appearance of extra lines on the X-ray films as criteria for a range of metal to oxygen stoichiometry. Thus the behavior of the NbO_2–NbO phase region is in complete agreement with most earlier studies.

The exception is the study of Shin, Halpern, and Raccah (*5*) who quote a stoichiometry range of from $NbO_{1.9}$ to $NbO_{2.10}$ for the dioxide phase. An examination of Table III shows that our samples were diphasic when

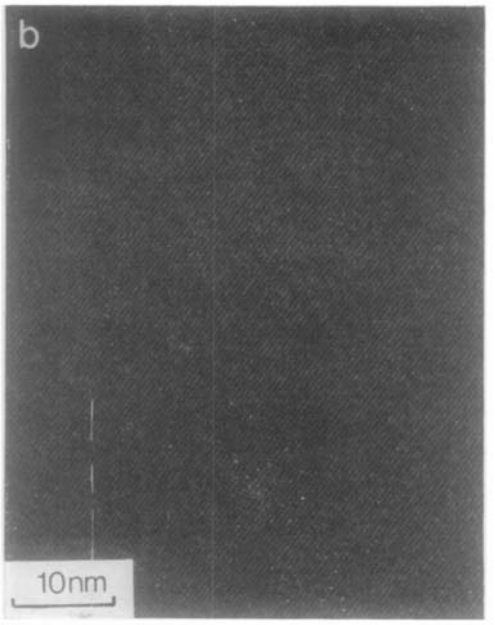

FIG. 9—*Continued*

well within this range. Coupled with the fact that the lattice parameters of the NbO_2 phase in our experiments did not vary significantly, we cannot draw any other conclusion than that the NbO_2 phase has a very narrow stoichiometry range at room temperature, although this might not be so at higher temperatures, (vide infra). The results of Shin, Halpern, and Raccah are therefore anomalous and do not agree with the bulk of data so far published, but the reason for this discrepancy is not apparent.

The most interesting observation in the present study is that the NbO_2 seems to change its symmetry towards that of rutile in slightly reduced samples. Such a transformation certainly takes place at high temperatures (10–13) and has been associated with a separation of the Nb–Nb pairs that occurs in the room-temperature phase. A similar change to the rutile structure occurs if foreign cations are doped into NbO_2 to produce $(Nb_xM_{1-x})O_2$. Thus the Nb–Nb bonds appear to be fairly easily disrupted and this disruption leads naturally to the formation of a rutile structure.

In the present case, impurities do not appear to be responsible for the transformation observed. The starting materials were of high purity and the presence of faulting in the prepared samples was always coincident with the presence of NbO in the material, that is, with an overall drop in the metal to oxygen ratio from 2.00. Substantial impurity effects would have been expected to also cause the stoichiometric NbO_2 to transform, at least partially, to a rutile structure or to the faulted modification.

The effect therefore seems to be associated with a drop in stoichiometry to below 2.00, which in turn influences the degree of Nb–Nb bonding, perhaps in a similar way to that produced by either temperature or impurities. Although the homogeneity range of NbO_2 appears to be very narrow at room temperature, it may become somewhat broader at the higher temperatures involved in reaction and may therefore allow NbO_2 to vary somewhat in composition to $NbO_{2-\delta}$ when in samples of overall composition of less than $NbO_{2.0}$. Upon cooling one could envisage that this would revert to almost stoichiometric NbO and NbO_2, resulting in a precipitate of NbO in the NbO_2 matrix. Such areas are often seen in samples with overall compositions close to $NbO_{1.6}$, and in all such areas the NbO_2 has an unfaulted microstructure.

The formation of NbO in a matrix of NbO_2 will clearly involve significant nucleation energies. An alternative procedure which may be preferable would be a complete or partial unmixing of the slightly substoichiometric high-temperature phase into bands of NbO_2 and NbO_{2-x} with the rutile structure. Contrast effects observed in systems where spinodal or similar unmixing has taken place are quite similar to those observed here (*28*, *30*). As would be expected in such unmixing, annealing sharpens the boundaries between the "phases" making them more readily visible by diffraction contrast. The intermediate structure of the $P4_1$ type could then represent either a transitional structure between the $I4_1/a$ and $P4_2/mnm$ (rutile) forms or, alternatively, a modification with a slightly different tolerance for oxygen deficiency.

The fact that the boundaries between the various modifications of the NbO_2 structure are not strictly along $\{h00\}$ or $\{0k0\}$ suggests

that some strain-releasing mechanism may be taking place similar to that observed before in twinned V_2O_5 (*31*). This energy term would become more important as the gross departure from stoichiometry increases, and when this becomes too great to tolerate the nucleation of NbO in a matrix of NbO_2 may then occur.

In conclusion one can say that the microstructural form of materials with compositions between NbO and NbO_2 has been clarified and in this system crystallographic shear does not appear to be important. However, a slightly substoichiometric form of NbO_2 may exist at high temperatures and further studies of how this phase unmixes on cooling and annealing, and of the diffraction effects associated with the texture of these faulted samples, would be of interest.

Note added in proof. Since this paper was completed two further reports on NbO_2 have come to our attention. In the first Marucco *et al.* (*32*) examined the stoichiometry range of NbO_2 very carefully. They found no evidence for any appreciable composition range below $NbO_{2.00}$ and only a small composition range (of the order of $NbO_{2.005}$ at 1323°K) on the oxygen-rich side. The second report, by Pynn *et al.* (*33*), discusses the structure of the low-temperature form of NbO_2. They find the same space group as that reported by Marinder (*9*). Both of these reports are concerned with fully oxidized NbO_2 and do not refer to the slightly reduced material described in the paper above, but they are of some importance in the light of the discussions of stoichiometry and structure made in the paper.

Acknowledgments

We are indebted to the Science Research Council for an equipment grant and for financial support to J.R.G., and to Professor D. Bijl for his interest and encouragement in this study.

References

1. G. BRAUER, *Z. Anorg. Allg. Chem.* **248**, 24 (1941).
2. R. P. ELLIOT, *Trans. Amer. Soc. Met.* **52**, 990 (1960).
3. N. TERAO, *Japan J. Appl. Phys.* **2**, 156 (1963).
4. J. NIEBUHR, *J. Less-Common Metals* **11**, 191 (1966).
5. S. H. SHIN, T. H. HALPERN, AND P. M. RACCAH, *Mat. Res. Bull.* **10**, 1061 (1975).
6. S. ANDERSSON AND L. JAHNBERG, *Ark. Kemi* **21**, 413 (1963).
7. L. A. BURSILL AND B. G. HYDE, "*Progress in Solid State Chemistry*" (H. Reiss and J. O. McCaldin, Eds.), Vol. 7, Pergamon, Oxford (1972).
8. A. MAGNÉLI, G. ANDERSSON, AND G. SUNDKVIST, *Acta Chem. Scand.* **9**, 1402 (1955).
9. B.-O. MARINDER, *Ark. Kemi* **19**, 435 (1962).
10. T. SAKATA, K. SAKATA, AND I. NISHIDA, *Phys. Status Solidi* **20**, K155 (1967).
11. T. SAKATA, *J. Phys. Soc. Japan*, **26**, 582 (1969).
12. H. SCHÄFER, D. BERGNER, AND R. GRUEHN, *Z. Anorg. Allg. Chem.* **365**, 31 (1969).
13. S. M. SHAPIRO, J. D. AXE, G. SHIRANE, AND P. M. RACCAH. *Solid State Commun.* **15**, 377 (1974).
14. K. SAKATA, *J. Phys. Soc. Japan*, **26**, 867 (1969).
15. R. F. JANNINCK AND D. H. WHITMORE, *J. Phys. Chem. Solids* **27**, 1183 (1966).
16. J. A. ROBERSON AND R. A. RAPP, *J. Phys. Chem. Solids* **30**, 1119 (1969).
17. T. SAKATA AND E. FROMM, *Z. Anorg. Allg. Chem.* **398**, 129 (1973).
18. C. N. R. RAO, G. R. RAO, AND G. V. SUBBA RAO, *J. Solid State Chem.* **1**, 340 (1973).
19. G. BELANGER, J. DESTRY, G. PERLUZZO, AND P. M. RACCAH, *Can. J. Phys.* **52**, 2272 (1974).
20. G. ANDERSSON AND A. MAGNÉLI, *Acta Chem. Scand.* **11**, 1065 (1957).
21. A. L. BOWMAN, T. C. WALLACE, J. L. YARNELL, AND R. G. WENZEL, *Acta Crystallogr.* **21**, 843 (1966).
22. E. R. POLLARD, unpublished results quoted by G. V. CHANDRASHEKAR, J. MOYS, AND J. M. HONIG, *J. Solid State Chem.* **2**, 528 (1970); J. M. HONIG, W. E. WAHNSIEDLER, AND P. C. EKLUND, *J. Solid State Chem.* **6**, 203 (1973).
23. C. B. ALCOCK, S. ZADOR, AND B. C. H. STEELE, *Proc. Brit. Ceram. Soc.* No. 8, 231 (1967).
24. P. E. WERNER, *Arkiv. Kemi* **31**, 513 (1969); *Chem. Comm. Univ. Stockholm* No. XV (1973).
25. N. NORIN, *Acta Chem. Scand.* **17**, 1391 (1963).
26. P. B. HIRSCH, A. HOWIE, R. B. NICHOLSON, D. W. PASHLEY, AND M. J. WHELAN, "Electron Microscopy of Thin Crystals," Chap. 14, Butterworths, London (1965).
27. A. J. C. WILSON, "X-Ray Optics," 2nd Ed., Methuen, London (1962).
28. J. D. C. MCCONNELL, *Philos. Mag.* **11**, 1289 (1965); **19**, 221 (1969); *Min. Mag.* **38**, 1 (1971).
29. J. M. COWLEY, "Diffraction Physics," North-Holland, Amsterdam (1975).
30. A. H. SCHULTZ AND V. S. STUBICAN, *Philos. Mag.* **18**, 929 (1968).
31. R. J. D. TILLEY AND B. G. HYDE, *Phys. Status Solidi* **A2**, 749 (1970).
32. J. F. MARUCCO, R. TETOT, P. GERDANIAN, AND C. PICARD. *J. Solid State Chem.* **18**, 97 (1976).
33. R. PYNN, J. D. AXE, AND R. THOMAS, *Phys. Rev. B* **13**, 2965 (1976).